

Supplementary Fig. 1. Ubiquitin-dependent transient recruitment of the p97 segregase to UV lesions.

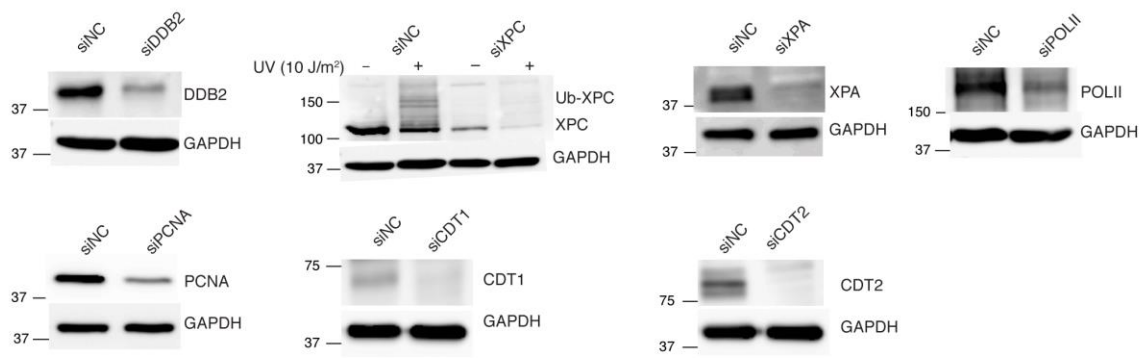
(a) Endogenous p97 of U2OS cells was monitored during 24 hours after inflicting local UV damage by irradiation (100 J·m⁻²) through the pores of a micropore filter. Scale bar, 10 μm.

(b) Quantification of p97 accumulation at UV lesions spots over two independent

experiments (>200 nuclei); error bars, s.e.m. (c) The proteasome inhibitor MG132 (10 μM, 5

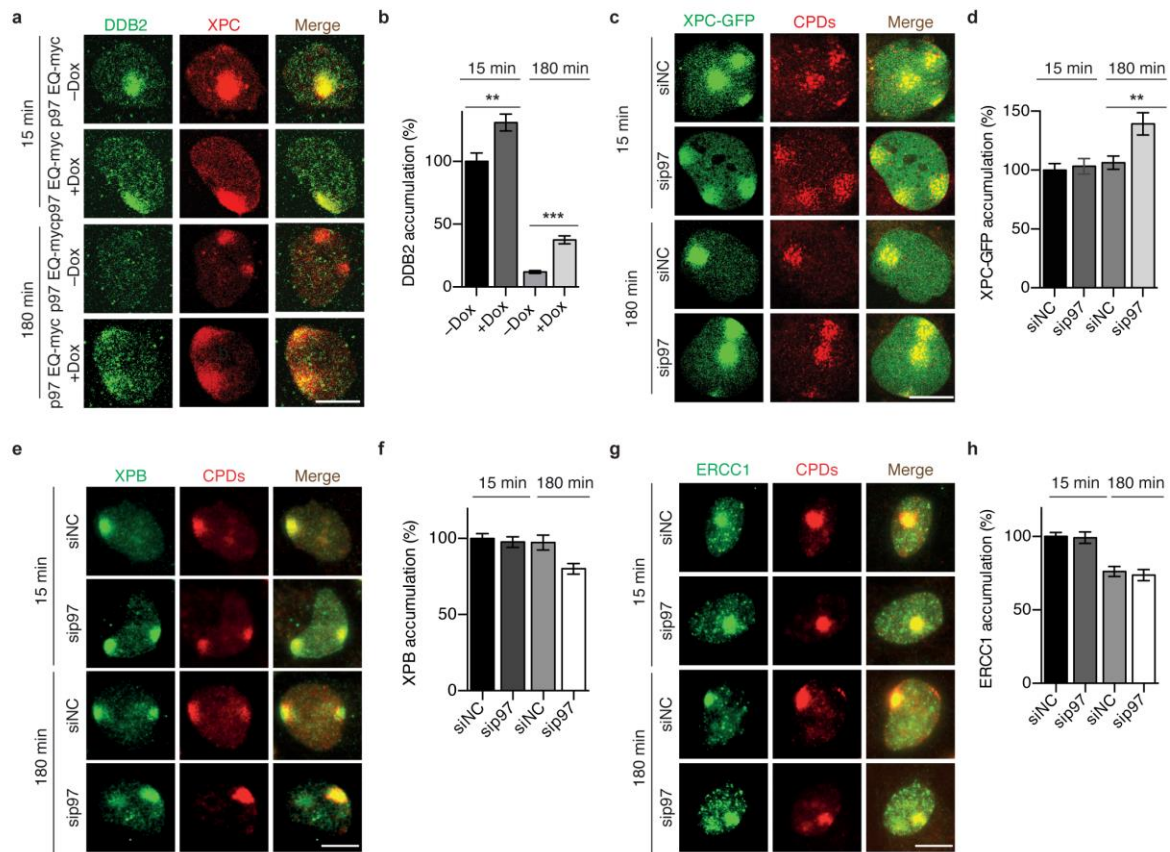
h) depletes the nuclear pool of free ubiquitin, as demonstrated earlier¹. This effect is

illustrated for XPC protein, which due to the MG132 treatment fails to be ubiquitinated in U2OS cells following whole-cell UV irradiation ($10 \text{ J}\cdot\text{m}^{-2}$). The location of molecular weight markers (in kDa) is indicated for each blot. **(d)** Immunoblot analysis of cell lysates demonstrating the efficiency of siRNA-mediated down regulation of Cul3, Cul4A and p97. **(e)** Cul4A is the major E3 ubiquitin ligase for the recruitment of p97 EQ to UV lesions. U2OS cells were transfected with siRNA targeting the indicated cullins 72 h before induction of UV spots, and the cells were probed for CPD formation and p97 EQ recruitment 15 min after irradiation; siNC, non-coding siRNA control. Scale bar, 10 μm . **(f)** Quantification of p97 EQ at UV spots over three independent experiments (>300 nuclei); error bars, s.e.m., $***P<0.001$ relative to siNC control (unpaired two-tailed t -test).



Supplementary Fig. 2. DDB2 is a main substrate for the p97 protein segregase.

Immunoblot analysis of U2OS cell lysates demonstrating the efficiency of siRNA-mediated down regulation of DDB2, XPC (under unchallenged conditions and after UV irradiation, as indicated), XPA, POLII, PCNA, CDT1 and CDT2. GAPDH, glyceraldehyde 3-phosphate dehydrogenase used as a loading control.



Supplementary Fig. 3. The p97 segregase controls the cellular homeostasis of DDB2 and XPC but not the downstream NER factors XPB and ERCC1.

(a) Chromatin retention of DDB2 and XPC visualised in U2OS cells 15 and 180 min after inflicting UV damage spots by irradiation through micropore filters. Mild expression of the dominant-negative p97 EQ mutant was induced by doxycycline (+ Dox). Scale bar, 10 μ m.

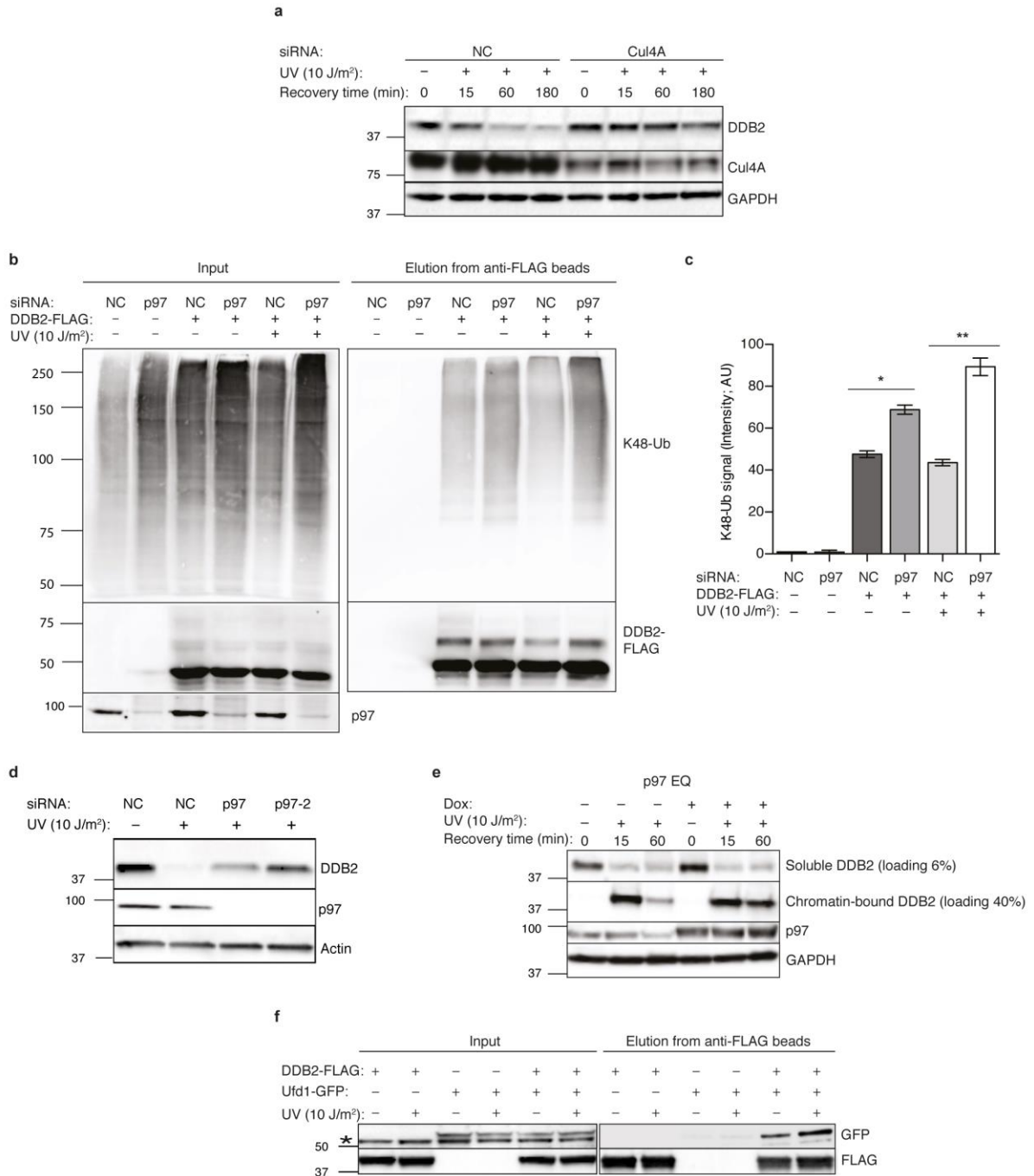
(b) Quantification of DDB2 in chromatin, as illustrated in panel (a), over three independent experiments (>300 nuclei). Error bars, s.e.m.; *** P <0.001, ** P <0.01 (unpaired two-tailed t -test).

(c) Retention of a poorly ubiquitinated XPC-GFP fusion in chromatin. U2OS cells were treated with siRNA as indicated (for 72 h before local UV irradiation) and transfected with an expression vector for XPC-GFP (18 h before irradiation); siNC, non-coding RNA control. (d)

Quantification of XPC-GFP in chromatin, as illustrated in panel (c), over three independent experiments (>300 nuclei). (e, f) Chromatin retention of XPB is not increased upon depletion

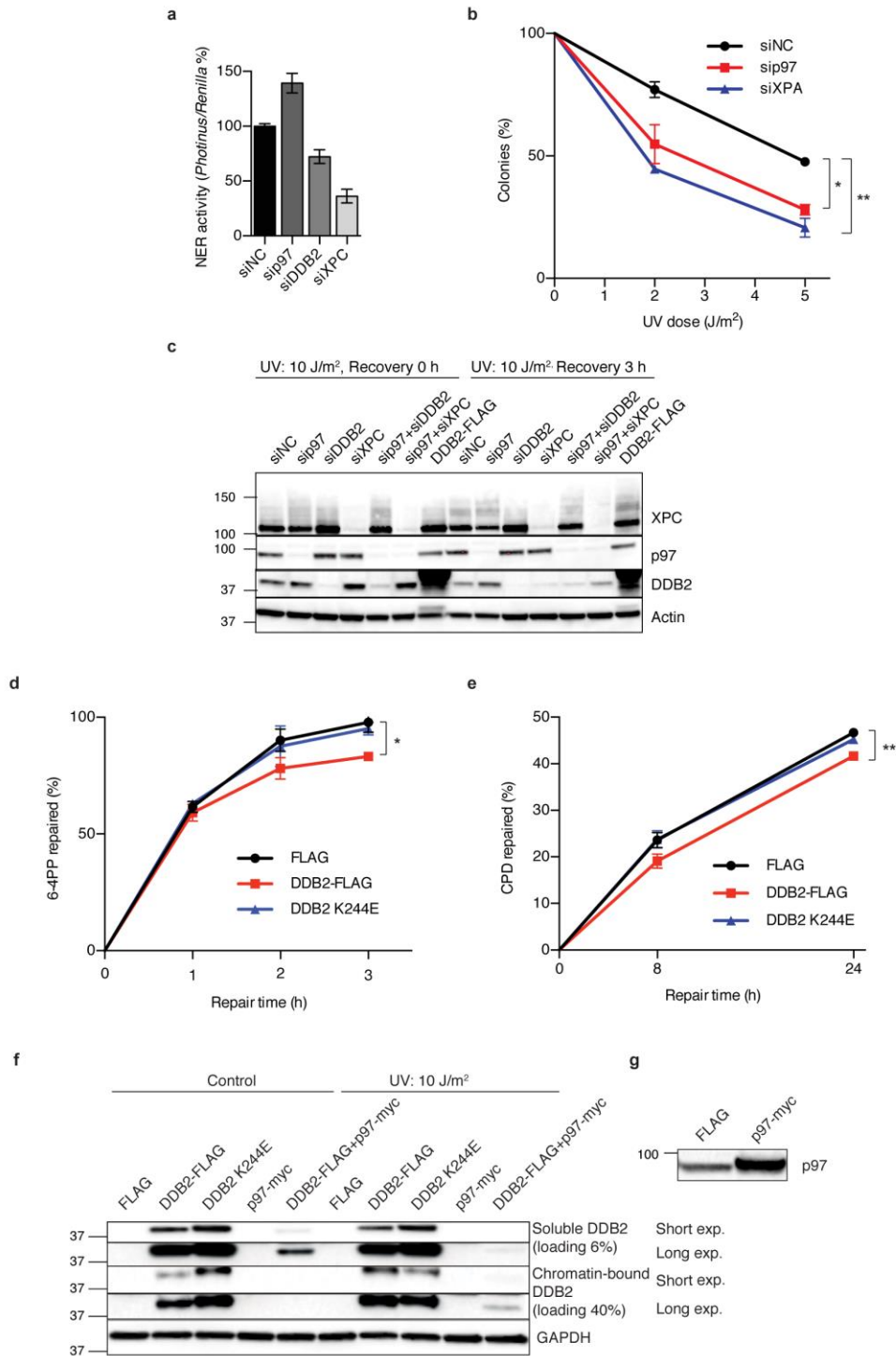
of p97; quantifications were carried out over two independent experiments (>200 nuclei). (**g**,

h) Chromatin retention of ERCC1 is not altered upon depletion of p97; quantifications were carried out over two independent experiments (>200 nuclei).



Supplementary Fig. 4. Degradation of K48-ubiquitinated DDB2 is Cul4A- and p97-Ufd1-Npl4-dependent. (a) UV-dependent degradation of DDB2 is suppressed by Cul4A depletion. U2OS cells were depleted of Cul4A by siRNA treatment for 72 hours. Cells were UV irradiated and degradation of DDB2 was monitored 3 hours after UV exposure. NC, non-coding siRNA control. (b) Increased ubiquitination of DDB2 following suppression of p97.

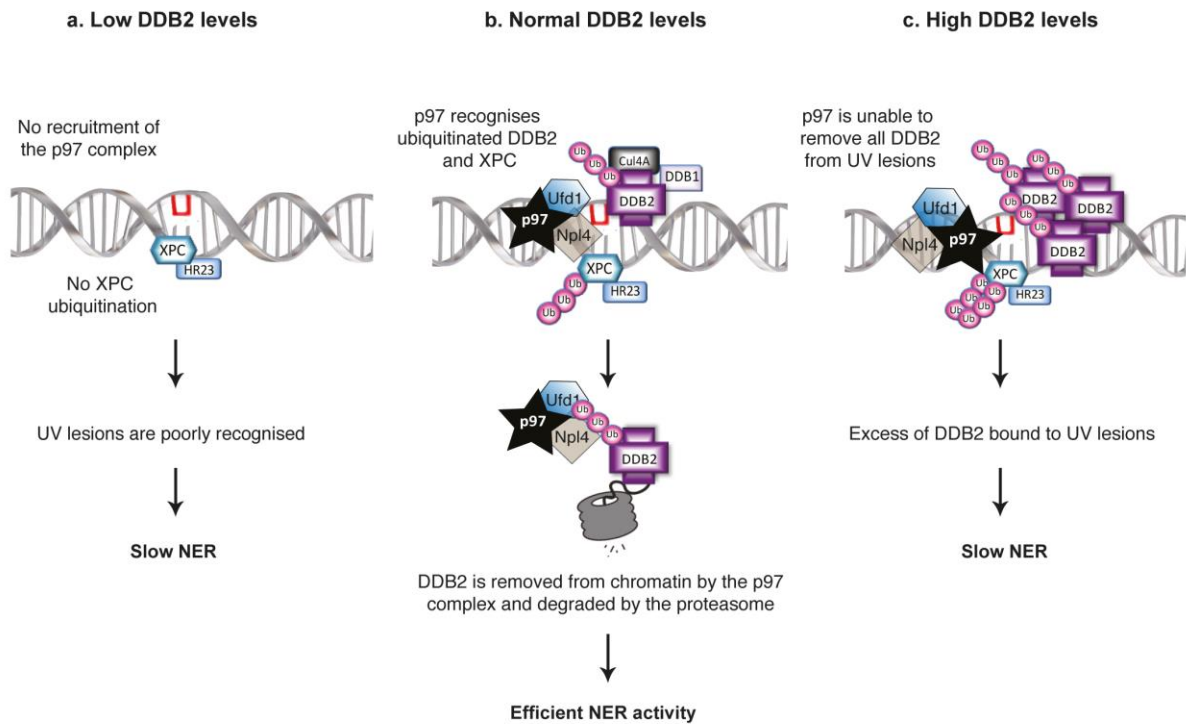
HEK cells were treated with siRNA (72 h), transfected with an expression vector for DDB2-FLAG and UV-irradiated as indicated. After cell lysis under denaturing conditions, immunoprecipitation was carried out using beads coated with anti-FLAG antibodies. Analysis of the resulting eluates demonstrated an accumulation of K48-ubiquitin-modified DDB2 following p97 depletion. **(c)** Quantification of K48-ubiquitin-modified DDB2-FLAG over three independent experiments. Significance was determined after normalisation to non-modified DDB2-FLAG. Error bars, s.e.m.; ** $P < 0.01$ and * $P < 0.05$ (unpaired two-tailed *t*-test). **(d)** Inhibition of UV-induced DDB2 degradation in U2OS cells demonstrated with two distinct siRNA sequences targeting p97. The siRNA reagent designated “p97” is used in the experiments of Figures 1, 3 and 5 of the main text. Whole-cell lysates were probed by immunoblotting 3 h after UV irradiation. **(e)** Inhibition of UV-induced DDB2 degradation in U2OS cells following mild expression of the dominant-negative p97 EQ mutant. Dox, doxycycline used for p97 EQ induction. DDB2 bound to chromatin was compared with the respective level in the non-chromatin-bound (“soluble”) fraction. **(f)** p97 adaptor Ufd1 is present in a DDB2 protein complex. HEK cells were transfected with expression vector for DDB2-FLAG and Ufd1-GFP and UV-irradiated as indicated. After cell lysis, immunoprecipitation was carried out using beads coated with anti-FLAG antibodies. Analysis of the resulting eluates demonstrated Ufd1 in the same complex with DDB2. The asterisk indicates a non-specific band, generated by cross-reactivity, which was identified in the input mixtures containing no GFP.



Supplementary Fig. 5. Down regulation of p97 causes hypersensitivity to UV light and chromosomal aberrations by disrupting DDB2 and XPC homeostasis.

(a) Host-cell reactivation of a luciferase reporter vector in HeLa cells treated with siRNA targeting the indicated proteins; siNC, non-coding control RNA. The assay was repeated

three times in triplicates; error bars, s.e.m. In this test based on a non-chromatinised DNA substrate, depletion of p97 resulted in slight stimulation of NER activity. **(b)** Colony forming assay demonstrating that p97-depleted HeLa cells (by treatment with siRNA targeting p97) are hypersensitive to killing by UV radiation (n=3, each measurement in triplicate). The error bars indicate s.e.m. (** $P < 0.01$ and * $P < 0.05$ using the unpaired two-tailed t -test). **(c)** Whole-cell level of the indicated proteins after siRNA treatment (72 h) of HEK cells. In part, the cells were transfected with a vector for expression of DDB2-FLAG as indicated. **(d, e)** Excess of DDB2 but not of the K244E mutant, resulting from transfection of HeLa cells with the respective expression vectors, slows down repair of 6-4PP and CPDs (n=4, each measurement in duplicate). The error bars indicate s.e.m. (** $P < 0.01$ and * $P < 0.05$ using the unpaired two-tailed t -test). **(f)** Levels of DDB2 protein bound to chromatin and in the non-chromatin (“soluble”) fraction of HEK cells after over-expression of p97-myc, as indicated. The samples for immunoblotting were collected before UV irradiation and 3 h after irradiation. **(g)** Over-expression of p97-myc in HEK cells. The control lane (“FLAG”) shows the normal level of endogenous p97 in cells transfected with a vector coding for the FLAG epitope. The lane indicated with “p97-myc” illustrates the increased p97 level induced by transfection with the respective expression vector. The blot was probed with anti-p97 antibodies.



Supplementary Fig. 6. Model illustrating how DDB2 levels, regulated by the p97

segregase complex, impact on NER efficiency. (a) In the absence of DDB2, UV lesions are poorly recognized and their excision is slow. Also, XPC is not ubiquitinated and the p97 complex is not recruited to UV lesion sites. (b) Efficient global-genome NER activity requires both normal levels of DDB2 and the p97-dependent removal of this damage sensor from its DNA substrate in chromatin. (c) Conversely, excessive levels of DDB2 on the DNA substrate in chromatin lead to impaired NER activity and, as a consequence, to genome instability.

Figure 2c

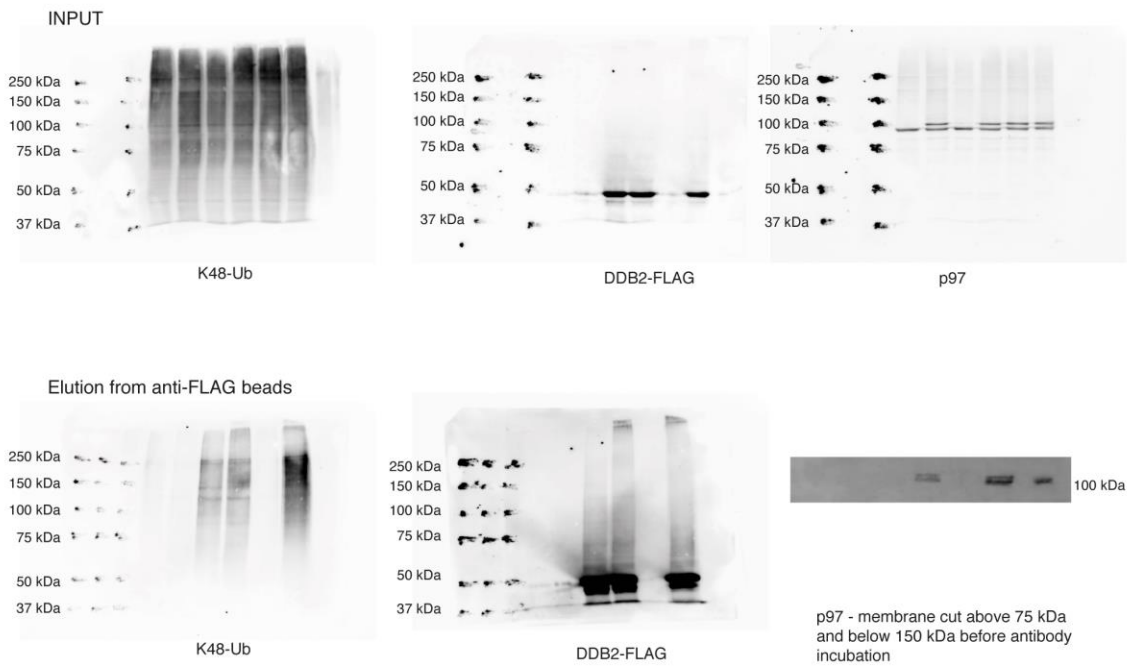
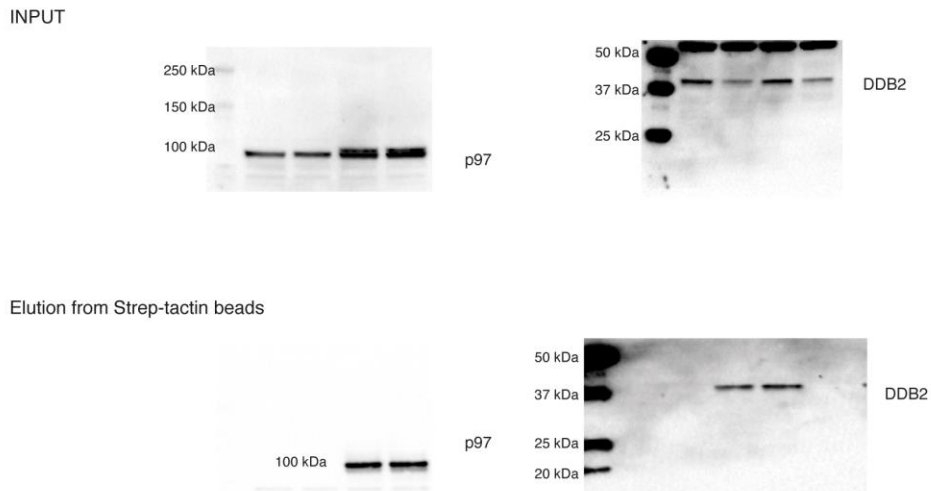


Figure 2d



Supplementary Fig. 7. Full blots of Fig. 2, as indicated.

Figure 3d

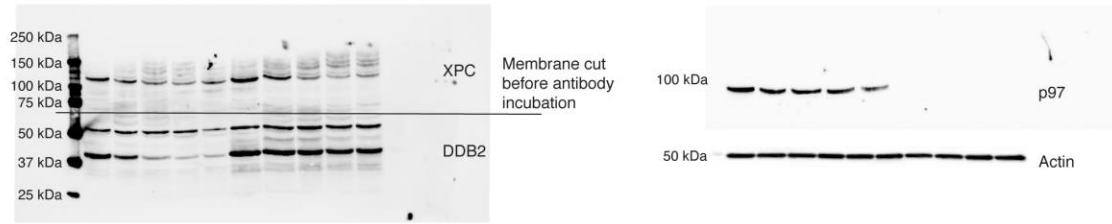


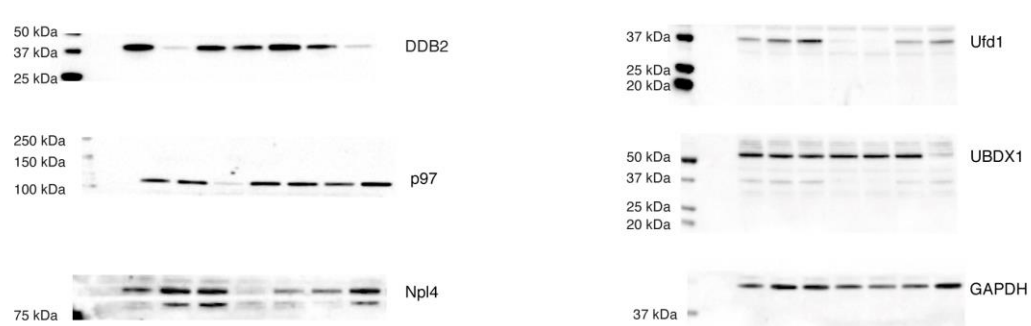
Figure 3e



Figure 4c



Figure 4d



Supplementary Fig. 8. Full blots of Fig. 3 and Fig. 4, as indicated.

Supplementary Table 1. List of siRNA sequences in alphabetical order.

Target	Sequence	Source/reference
Non-coding	5'-AAUUCUCCGAACGUGUCACGU-3'	Qiagen, Cat. No. SI03650325
CDT1	5'-GCUGUUGUACUAUCAUGAGCCCUGGTT-3'	Microsynth ²
CDT2	5'-CAAUGGACACCAGAACUCUACCUUUTT-3'	Microsynth ³
Cul3	5'-AACAAACUUUCUCAAACGCTA-3'	Qiagen, Cat. No. SI02225685
Cul4A	5'-UUCGAAGGACAUCAUGGUUCA-3'	Qiagen, Cat. No. SI04245465
Cul4B	5'-CACCGUCUCUAGCUUUGCUAA-3'	Qiagen, Cat. No. SI03162215
DDB2	5'-GGAUCAAGCAGUUAUUUGATT-3'	Qiagen, Cat. No. SI02664823
DVC1	DVC1-1: 5'-GUCAGGAAGUUCUGGUUAATT-3'	Microsynth
	DVC1-2: 5'-CACGAUGAGGUGGAUGAGUAUTT-3'	Microsynth
NPL4	5' -CACGCCUAA UCCUGUUGACAA-3'	Qiagen ⁴ , Cat. No. SI04211382
PCNA	5'-ATGGATTTAGATGTTGAACAA-3'	Qiagen, Cat. No. SI1027415
POLII	5'-GCGGCUUCAGCCCAGGUUATT-3'	Qiagen, Cat. No. SI04354420
UBXD1	5'- CGCCTCCATCATGAAGATCTA-3'	Qiagen, Cat. No. SI04209044
UBXD7	5'-CAGCACGTGCATATTCATTTA-3'	Qiagen, Cat. No. SI00455364
UFD1	5'-CACTGGATGATGCAGAACTTA-3'	Qiagen, Cat. No SI04132583
p97	VCP7: 5'-AACAGCCAUUCUCAACAGAA-3'	Qiagen ⁵ , Cat. No. SI03019730
	VCP6: 5'-CCCAAGAUGGAUGAAUUGCAGUUGU-3'	Invitrogen ⁴ , Cat. No. HSS111263
XPA	5'-GCUACUGGAGGCAUGGCUATT-3'	Microsynth ⁶
XPC	5'-GCAA AUGGCUUCAUCGAATT-3'	Qiagen, Cat. No. SI00066227

Supplementary Table 2. List of antibodies with working dilutions.

Source/reference	Antibody	Dilutions
Abcam	Mouse anti-DDB2	1:50 for immunofluorescence microscopy 1:200 for protein immunoblotting
	Rabbit anti-Cul4A	1:1'000 for protein immunoblotting
	Mouse anti-PCNA	1:5'000 for protein immunoblotting
	Mouse anti-POLII	1:1'000 for protein immunoblotting
	Mouse anti-UFD1	1:300 for protein immunoblotting
	Mouse anti-VCP	1:250 for immunofluorescence microscopy
	Mouse anti-XPC	1:1'000 for protein immunoblotting
Ambion	Mouse anti-GAPDH	1:100'000 for protein immunoblotting
Bethyl	Rabbit anti-CDT1	1:1'000 for protein immunoblotting
	Rabbit anti-CDT2	1:2'000 for protein immunoblotting
	Rabbit anti-Cul3	1:2'000 for protein immunoblotting
Cell Signaling	Rabbit anti-c-myc	1:250 for immunofluorescence microscopy
	Rabbit anti- α -tubulin	1:50'000 for protein immunoblotting
Clontech	Rabbit anti-GFP	1:1'000 for protein immunoblotting
Cosmo Bio	Mouse anti-CPD	1:1'000 for immunofluorescence microscopy
	Mouse anti-6-4PP	1:1'000 for immunofluorescence microscopy
Invitrogen	Alexa Fluor 594 goat anti-mouse	1:400 for immunofluorescence microscopy
	Alexa Fluor 488 goat anti-mouse	1:400 for immunofluorescence microscopy
	Alexa Fluor 488 goat anti-mouse	1:400 for immunofluorescence microscopy
	Alexa Fluor 594 goat anti-mouse	1:400 for immunofluorescence microscopy
Millipore	Rabbit anti-Ub-K48 clone Apu2	1:100 for immunofluorescence microscopy, 1:500 for protein immunoblotting
	Rabbit anti-UBXD1	1:1'000 for protein immunoblotting
Santa Cruz	Rabbit anti-c-myc A-14	1:250 for immunofluorescence microscopy
	Rabbit anti-ERCC1	1:50 for immunofluorescence microscopy
	Rabbit anti-XPA FL-273	1:100 for protein immunoblotting
	Rabbit anti-XPB	1:100 for immunofluorescence microscopy
Sigma	Mouse anti-FLAG M2	1:4'000 for protein immunoblotting
	Rabbit anti-DVC1	1:1'000 for protein immunoblotting
	Rabbit anti-Npl4	1:250 for immunoblotting
	Rabbit anti-XPC	1:100 for immunofluorescence microscopy
	peroxidase anti-mouse and anti-rabbit IgG	1:20'000 for protein immunoblotting
Ref. 5	Rabbit anti-p97	1:2'000 for protein immunoblotting

References

1. Dantuma, N. P., Groothuis, T. A., Salomons, F. A. & Neeffjes, J. A dynamic ubiquitin equilibrium couples proteasomal activity to chromatin remodeling. *J. Cell Biol.* **173**, 19-26 (2006).
2. Sugimoto, N. *et al.* Cdt1 phosphorylation by cyclin A-dependent kinases negatively regulates its function without affecting geminin binding. *J. Biol. Chem.* **279**, 19691-19697 (2004).
3. Raman, M., Havens, C. G., Walter, J. C. & Harper, J. W. A genome-wide screen identifies p97 as an essential regulator of DNA damage-dependent CDT1 destruction. *Mol. Cell* **44**, 72-84 (2011).
4. Meerang, M. *et al.* The ubiquitin-selective segregase VCP/p97 orchestrates the response to DNA double-strand breaks. *Nat. Cell Biol.* **13**, 1376-1382 (2011).
5. Ramadan, K. *et al.* Cdc48/p97 promotes reformation of the nucleus by extracting the kinase Aurora B from chromatin. *Nature* **450**, 1258-1262 (2007).
6. Staresinic, L. *et al.* Coordination of dual incision and repair synthesis in human nucleotide excision repair. *EMBO J.* **28**, 1111-1120 (2009).